(Received 10 December 2024, Accepted 26 December 2024, Scheduled 5 January 2025)

Performance Analysis of Plasmonic Sensor Modified with Chitosan-Graphene Quantum Dots Based Bilayer Thin Film Structure for Real-Time Detection of Dopamine

Faten Bashar Kamal Eddin[1, 2], Yap Wing Fen[3, 4, *], Ke Cui[2], Josephine Ying Chyi Liew[3], Hong Ngee Lim[5], Nurul Illya Muhamad Fauzi[4], Wan Mohd Ebtisyam Mustaqim Mohd Daniyal[4], and Saimei Hou[2]

[1] *Centre for Optical and Electromagnetic Research, College of Optical Science and Engineering Zhejiang University, Hangzhou 310058, China*
[2] *Zhejiang Engineering Research Center for Intelligent Medical Imaging Sensing and Non-invasive Rapid Testing, Taizhou Hospital, Zhejiang University, Taizhou, China*
[3] *Department of Physics, Faculty of Science, Universiti Putra Malaysia (UPM), Serdang, Selangor 43400, Malaysia*
[4] *Functional Nanotechnology Devices Laboratory, Institute of Nanoscience and Nanotechnology (ION2) Universiti Putra Malaysia (UPM), Serdang, Selangor 43400, Malaysia*
[5] *Department of Chemistry, Faculty of Science, Universiti Putra Malaysia (UPM), Serdang, Selangor 43400, Malaysia*

ABSTRACT: The performance of surface plasmon resonance (SPR) sensor modified with chitosan-graphene quantum dots (CS-GQDs)/Au bilayer thin film for dopamine (DA) detection was evaluated in this work. The sensor's selectivity to DA was evaluated in the presence of various interfering substances. The sensor's stability was examined over three weeks. Additionally, the repeatability of this sensor was assessed through nine successive measurements, and its reproducibility was evaluated using six different sensor films. The sensor demonstrated excellent selectivity to DA when 1 pM of DA was introduced to a 100 pM mixture of epinephrine, ascorbic acid, and uric acid. Furthermore, the storage stability of the sensor was found to be excellent. The sensor showed good repeatability as well as reproducibility with relative standard deviation (RSD) values of 0.343% and 0.229%, respectively while detecting 1 fM of DA. The real-time DA detection showed that obtained response signals were stable after roughly 10 minutes of injection of all concentrations. By fitting the experimental data to Pseudo-first-order (PFO) kinetic model, the equilibrium SPR angular shift was 0.318° with adsorption rate constant of $0.240\,\mathrm{min}^{-1}$ for 1 fM DA contacting the sensor surface. AFM images revealed that DA influenced the surface morphology of the sensor film, changing its average roughness by 0.710 nm, and FTIR spectra showed changes in the spectral bands and peaks intensities. These findings showed that CS-GQDs/Au based SPR sensor is an advantageous option for rapidly and economically diagnosing DA deficiency with high selectivity and sensitivity.

1. INTRODUCTION

Recently, due to advances in science and technology, the development of highly sensitive biosensing techniques has shown impressive progress. Plasmonic-based biosensor, in particular, is an essential technology that allows for the miniaturization of biosensors, increasing detection throughput and lowering operational costs [1–4]. Plasmonic biosensors use plasmonic phenomena such as surface plasmon resonance (SPR) [5–10], localized SPR (LSPR) [11–13], surface enhanced Raman scattering (SERS) [14, 15], surface enhanced infrared absorption spectroscopy (SEIRAS) [16, 17], and surface-enhanced fluorescence (SEF) to detect analytes [18, 19]. Among these plasmonic-based approaches, sensing platforms based on SPR offer the ability to detect biomolecules in a fast, highly sensitive, and label-free manner. It can detect small variations in refractive index that result from the interactions between the SPR chip's surface and the target [20–29]. Furthermore, the binding kinetics at the surface can also be studied in realtime [30–35]. The most significant characteristics for assessing an SPR sensor's performance are its sensitivity, selectivity, stability, repeatability, reproducibility, and detection limit [36, 37].

However, one of the key obstacles in employing SPR sensors is detecting biological and chemical entities with extremely low concentrations or with low molecular weight. This disadvantage may be effectively overcome by using sensitivity enhancement methods. The modification of the SPR sensor's bare metallic film with gold nanoparticles (Au NPs) can significantly improve sensor sensitivity due to the combined impact of increased surface area and the electromagnetic coupling between the sensor film and Au NPs [38–40]. In addition, using Au nanostructures and magnetic NPs as amplification labels in bio-recognition processes might increase the recognition components' refractive indices and thus enhance the sensitivity of the SPR sensor. Furthermore, utilizing multilayer thin film structures has proved efficiency in increasing SPR sensitivity for many applications [41, 42]. The effects of high refractive index thin layers, as well as the specific number of layers needed

* Corresponding author: Yap Wing Fen (yapwingfen@upm.edu.my).

to improve SPR sensor sensitivity and increase resonance angular shift, have been theoretically investigated, and numerous experiments were carried out using bimetallic layers of Ag and Au [43, 44], carbon-based nanostructures, polymers, and other materials to analyze the effect of the used layers on the limit of detection (LOD) of various targets with varying molecular weights and concentrations [45–55].

Dopamine (DA) is a crucial neurotransmitter in the central and peripheral neural systems of mammals. Abnormal DA concentrations in the human body may result in neurodegenerative disorders including schizophrenia, senile dementia, and Parkinson's disease [56–66]. DA coexists at extremely low concentrations in biological samples with interfering species such as electroactive ascorbic acid (AA), uric acid (UA), and epinephrine (EP) at relatively high concentrations [67–70]. Therefore, developing a sensitive and selective sensor for monitoring and detecting DA concentrations is necessary in order to aid in disease diagnosis and prevention. Dutta and co-workers electrodeposited crosslinked p-aminostyrene (PAS) polymer thin films on Au and ITO substrates for SPR determination of DA, achieving good reusability, selectivity, and sensitivity from picomolar to micromolar concentrations [71]. Kamali et al. developed an SPR sensor using Ag/GO nanocomposite, demonstrating excellent selectivity for DA, with distinct SPR absorbance peaks for AA and UA that differed from those for DA [72]. Raj et al. developed an SPR fiber optic sensor using green-synthesized Ag NPs, achieving a 0.2 μM detection limit, good selectivity, and a 6-minute response time [73]. Jiang et al. functionalized an SPR sensor with a conjugated polymer, enabling regeneration through reversible swelling. The sensor selectively detected DA, even in the presence of AA, glucose, and UA, with increased DA adsorption at higher concentrations, reducing detection time. It remained stable for at least 2 weeks [74]. Manaf and co-workers designed an SPR sensor with a coating structure of four layers based on platinum NPs for sensitive and selective DA measurements when AA, glucose, and lysine were present [75]. Jabbari et al. introduced an SPR biosensor for the direct detection of DA using laccase immobilized on a carboxymethyl dextran (CMD) surface of SPR chip. This biosensor demonstrated a lower LOD of 0.1 ng/mL and a linear range from 0.01 to 189 μg/mL, providing good sensitivity and specificity for DA. The amine-coupling method comprising N-ethyl-N'-(3-diethylaminopropyl) carbodiimide (EDC) and N-hydroxysuccinimide (NHS) maintained enzyme activity, and pH 5.6 optimization enhanced DA interaction. Molecular docking studies confirmed the strong binding where K_D was 48.545 nM, with minimal interference from compounds such as AA, urea, and L-dopa. However, compared to other enzyme-based DA sensors, this method does not significantly surpass existing approaches in terms of performance [76]. Building on advancements in DA detection, Wekalao and Mandela (2024) proposed a graphene metasurface-based SPR biosensor in the terahertz regime, achieving 500 GHz/RIU sensitivity and a 0.867 ppm detection limit. The sensor, optimized with machine learning through K-nearest neighbors (KNN) regression, outperformed conventional ones in detecting DA across concentrations from 10 to 0.001 ppm. However, selectivity was not reported, and further miniaturization and in vivo testing are needed for clinical applications [77]. Karki et al. (2024) developed an SPR biosensor with zinc oxide (ZnO) nanowires and cerium oxide (CeO_2) NPs for DA detection. The multi-layered sensor achieved a sensitivity of 95 deg/RIU and detected DA as low as 0.001 pM. While optimization improved sensitivity, selectivity tests were not conducted, leaving its performance in complex biological samples unaddressed [78]. Sharma et al. (2024) introduced a DA detection biosensor using a 2D material-assisted, LSPR-enhanced etched core mismatch optical fiber with Au NPs and GO coatings. The sensor demonstrated a sensitivity of 0.3842 nm/μM, linearity of 95.06%, and reproducibility at a DA concentration of 0.4 μM. Although the sensor showed strong potential for real-time DA monitoring, selectivity results were not provided [79]. Huang et al. recently developed an economical optical fiber SPR sensor with a hybrid structure of molybdenum disulfide nanosheets (MoS_2 NSs) and Au NPs using polydopamine-accelerated electroless plating. The sensor exhibited refractive index sensitivity ranging from 678.85 to 7231.64 nm/RIU, showing improvements of 52.35% and 16.37% over conventional sensors in low and high refractive index ranges. However, selectivity, stability, and reproducibility were not evaluated [80]. Despite these advancements, many DA sensors still face challenges related to selectivity, reproducibility, and the ability to detect DA at very low concentrations without interference from other biological species. Therefore, there is a need for further improvement in sensor design to address these issues.

In our previous works, chitosan-graphene quantum dots (CS-GQDs) nanocomposite thin film has been utilized and significantly enhanced the sensitivity of the developed SPR sensor to DA [81]. The proposed thin layer enabled the sensor to detect DA down to 1 fM which is the lowest LOD achieved for DA using SPR sensors [82–86]. Moreover, the effect of the adsorbed DA on both the thickness of the sensing layer and its optical properties was studied [87]. However, for more reliability of the appropriateness of the developed SPR sensor to detect DA, this CS-GQDs based SPR sensor still needs thorough evaluation of its efficiency in terms of selectivity, repeatability, reproducibility, and stability. In addition, the kinetic behaviour of DA solution that comes into contact with the sensor film should be studied. Furthermore, the reported studies did not use the structural measurements to investigate the behaviour of DA adsorption at the sensor film's surface. So, in this work, the selectivity tests of the developed CS-GQDs/Au based SPR sensor were conducted using samples including DA and other potentially interfering substances such as EP, AA, and UA. Additionally, the repeatability of this sensor was evaluated through many successive measurements, and the sensor reproducibility was assessed using different sensor films, while the sensor stability was tested over three weeks. The realtime detection of DA using this sensor was investigated by fitting the experimental results for different concentrations of DA interacted with CS-GQDs/Au sensor film to Pseudo-first-order (PFO) kinetic model. The structural analysis of the CS-GQDs/Au bilayer film was carried out to validate the adsorption of DA on the sensor layer, and the characterization was conducted both before and following DA injection, using Fourier transform infrared spectroscopy (FTIR) and the atomic force microscopy (AFM).

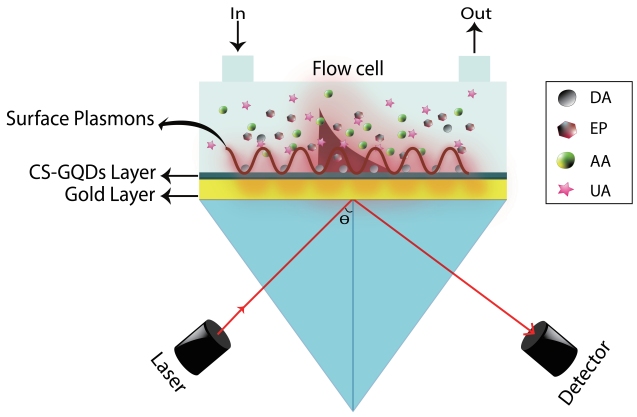

FIGURE 1. SPR spectroscopic system in Kretschmann configuration.

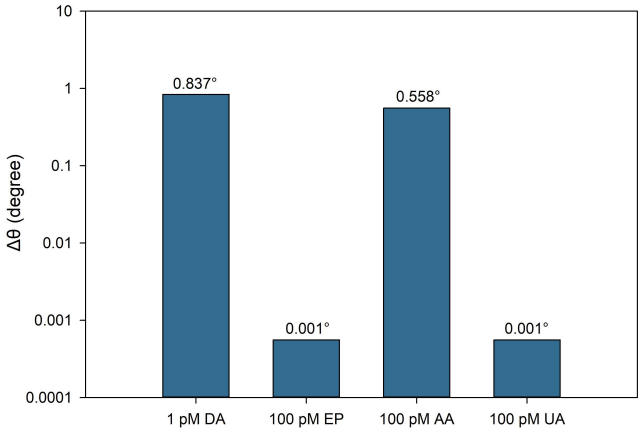

FIGURE 2. The angular shift response of CS-GQDs based sensor exposed to 1 pM DA, 100 pM of EP, AA, and UA separately.

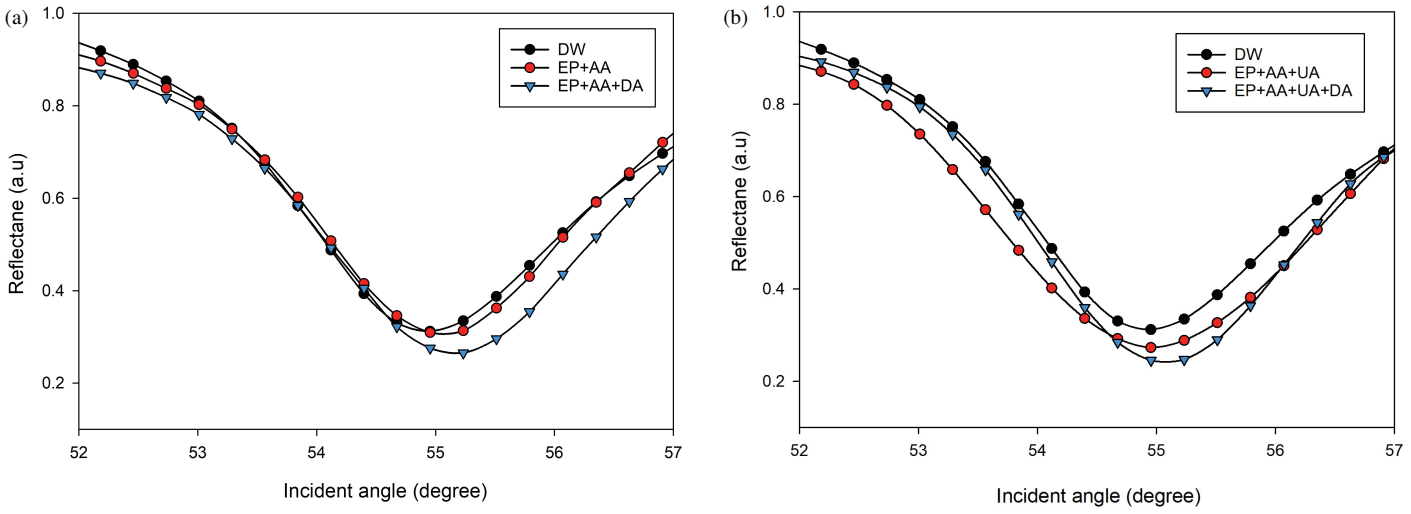

FIGURE 3. SPR reflectivity curves of CS-GQDs/Au bilayer film exposed to: (a) (EP, AA) and (EP, AA, DA) mixtures; (b) (EP, AA, UA) and (EP, AA, UA, DA) mixtures.

2. MATERIALS AND METHODS

2.1. Materials and Reagents

Graphene quantum dots with concentration of 1 mg/mL, medium molecular weight (MMW) CS, acetic acid (assay $\geq$ 99.7%), (-)-epinephrin (EP, MW = 183.20 g/mol), dopamine hydrochloride (DA, MW = 189.64 g/mol, powder), L-ascorbic acid (AA, MW = 176.12 g/mol, 99%), uric acid (UA, crystalline, MW = 168.11, $\geq$ 99%), and sodium hydroxide (NaOH, MW = 40 g/mol) were purchased from Sigma-Aldrich. Deionized water (DW) was used for dilution during the experiments. Menzel-Glaser, Germany provided a triangular prism with a refractive index of 1.7786, glass cover slips measuring 24 × 24 mm with thickness of 0.13–0.16 mm. Low viscosity index matching liquid (IML) with refractive index value of 1.52 at 589 nm was purchased from Norland (USA) to minimize the losses in reflection at the glass/air contact. The prism and cover slips were cleaned using acetone to ensure that their surfaces were free from contamination and any residual adsorbents that could impact the accuracy of the measurements.

2.2. Preparation of Target Solutions

Briefly, 50 mL of DW was used in order to dissolve 9.482 g of DA powder, resulting in a DA solution with a concentration of 1 M. EP solution of 0.5 M was obtained by using 5.58 g of EP to be dissolved in 50 mL of 0.1 M NaOH. The dissolution of 1.7612 g of AA in 20 mL of DW resulted in a 0.5 M of AA solution. Furthermore, 0.84055 g of the crystalline UA was dissolved in 47.5 mL of NaOH (0.1 M) to produce a UA solution of 100 mM. Then, DA, EP, AA, as well as UA solutions were diluted using DA to obtain extremely low levels down to 1 fM based on this formula ($M_1V_1 = M_2V_2$). Separate mixtures were also prepared, including (EP, AA), (EP, AA, UA), (EP, AA, DA) as well as (EP, AA, UA, DA) by combining equal amounts of DA (1 pM), and 100 pM of EP, UA, and AA.

2.3. Preparation of Sensor Chip

The glass cover slip was washed with acetone prior to depositing a 50 nm gold thin film on its surface using a Quorum Technologies Ltd K575X sputter coater (West Sussex, UK). The 50 nm Au layer was selected for its optimal balance between strong SPR signals and sharp resonance curves. This thickness is effective in coupling light to surface plasmons, providing the suitable penetration depth for surface interaction detection. A range of 45–65 nm is generally effective, as it ensures robust sensor performance with minimal impact on sensitivity [88, 89]. The sputtering was conducted with the target-substrate distance set to 25 mm and the gas pressure maintained at 5 psi. The coating process duration was 67 seconds, with a current 20 mA and voltage 2.2 kV. After getting the gold chips, the solution of the sensing layer (CS-GQDs) was prepared as explained by the authors in the previous work [76]. Lastly, 0.5 mL of that solution was carefully applied to the surface of the gold film. The sensor film (CS-GQDs/Au) was then deposited by spin coating for 30 seconds at 2000 rpm using a P-6708D spin coater.

2.4. Experimental Setup

The sensing capabilities of CS-GQDs/Au nanocomposite layer for detecting DA were investigated using a custom-built SPR spectroscopic system, set up in the Kretschmann configuration, as illustrated in Fig. 1. The system operated with the angular interrogation technique, incorporating a He-Ne laser of 632.8 nm, a light chopper, a linear polarizer, a pinhole, a prism, a flow cell, an optical programmable rotating platform, with a motion controller offering a resolution of 0.001°, alongside a photodetector and a lock-in amplifier. The SPR chips were securely bonded to the surface of the prism using the IML, and a flow cell holding the target solution was placed in touch with the SPR chip. This flow cell is a compact, custom-designed chamber constructed from durable materials. It ensures uniform analyte distribution across the SPR sensor surface for consistent interaction with the sensing layer. Its design features a well-aligned inlet and outlet to facilitate efficient analyte delivery while minimizing dead volume and ensuring consistent interaction with the sensing layer. The flow cell was securely sealed to prevent any leakage during measurements and was firmly mounted to maintain precise alignment with the prism and sensor surface.

Subsequently, SPR measurements were conducted in a dark environment. DW was introduced into the flow cell to contact the CS-GQDs/Au bilayer film generating the reference signal for the subsequent experiments. Following this, SPR measurements were carried out using a 1 fM DA solution. For this concentration of DA, the experiments were performed multiple times with the same sensing layer. Then, the sensing film was replaced many times while detecting 1 fM of DA. The measurements for 1 pM of DA were then performed using a new sensing film. Sequentially, SPR curves were recorded when the solutions of EP, AA, and UA at concentrations of 100 pM were injected separately into the cell to interact with the individual sensing films. Next, around 3 ml of each mixture (EP, AA), (EP, AA, DA), (EP, AA, UA), and (EP, AA, UA, DA) were sequentially introduced into the cell to record the SPR signals and assess the sensor's selectivity for DA.

2.5. Structural Analysis Techniques

FTIR spectra of CS-GQDs nanocomposite film, both before and after interactions with DA solution, were recorded in the range from 400 to 4000 cm^{-1} using ALPHA II FTIR Spectrometer in ATR mode Topographical measurements, and roughness analysis of the CS-GQDs films following DA interaction was conducted at room temperature with a Bruker Dimension Edge AFM, using a scanning size of 1 μm × 1 μm and PeakForce Tapping mode.

3. RESULT AND DISCUSSION

3.1. Selectivity of CS-GQDs/Au Based SPR Sensor

Previously, the ability of CS-GQDs/Au based SPR sensor to detect DA at 1 fM concentration was demonstrated [81]. Herein, SPR experiments showed that the response of this sensor to 1 pM DA was greater than its response to 100 pM of EP, AA, and UA samples when they were tested individually, where the SPR angular shift was 0.837° from the baseline for 1 pM of DA contacting the nanocomposite film 0.558° for 100 pM of AA while it was around 0.001° in case of 100 pM of UA and EP when tested separately as shown in Fig. 2. This indicates that this CS-GQDs/Au based SPR sensor is more sensitive to DA than other analytes. This aligns with Kamali et al. [72], who reported selectivity for DA using Ag/GO nanocomposites, but our sensor achieved a significantly lower LOD of 1 fM.

Figure 3(a) depicts SPR reflectance curves of the CS-GQDs/Au bilayer film exposed to a mixture of 100 pM AA and EP, both in the absence and presence of DA. It is obvious that adding 1 pM of DA to the (AA, EP) mixture led the SPR dip to shift by 0.280°. In addition, as shown in Fig. 3(b), the sensor film's responsiveness were enhanced after adding the same concentration of DA (1 pM) to the mixture of AA, UA, and EP in equal volumes. This demonstrates the high selectivity of the proposed sensor to DA, as it can effectively detect DA even in the presence of high concentrations of other potential interfering substances. These results can be attributed to the specific and quantitative interaction of DA with the sensor surface, which is influenced by the distinct structural characteristics of DA compared to the interfering substances, such as AA and UA. The sensor's selectivity for DA is largely determined by the molecular recognition of DA's unique functional groups, enabling more specific binding to the CS-GQDs/Au sensor surface. DA contains a primary amine group ($-NH_2$) that forms a stronger and more specific interaction with the sensor material, allowing it to bind more effectively than other substances like AA or UA, which do not possess similar functional groups. Furthermore, the sensor shows greater selectivity for DA over EP, likely due to the presence of a primary amine group in DA, in contrast to the methylated amine group in EP. DA synthesis starts with tyrosine through two main enzymatic steps: hydroxylation by tyrosine hydroxylase (TH) and decarboxylation by aromatic amino acid decarboxylase (AADC). The resulting DA

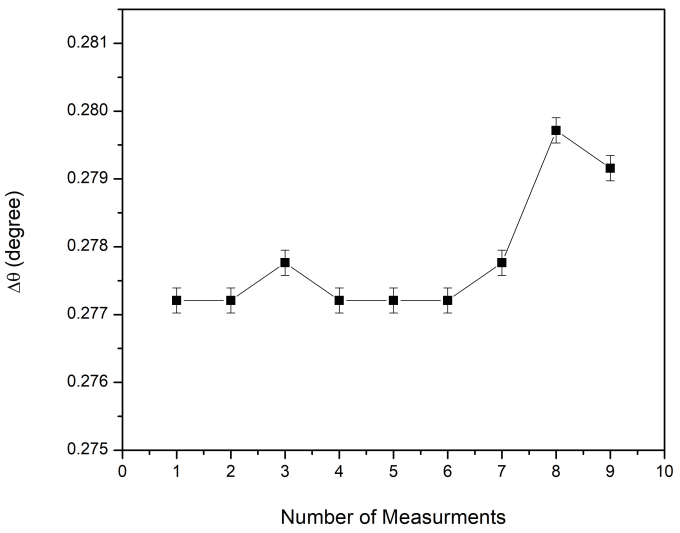

FIGURE 4. Assessment of the repeatability performance of the CS-GQDs based sensor.

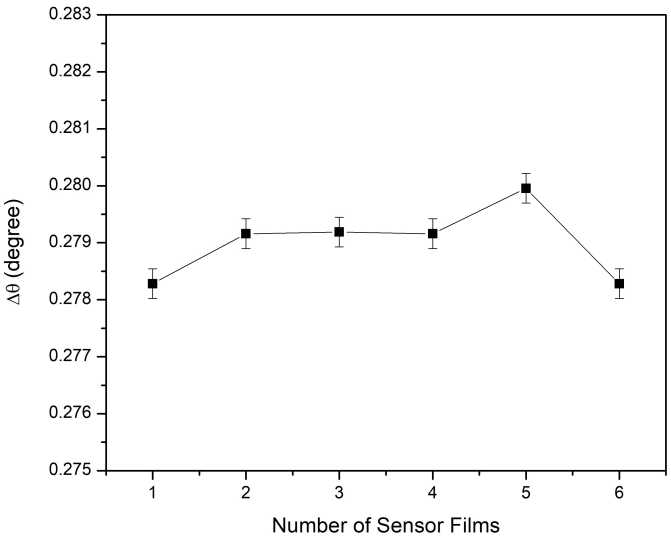

FIGURE 5. The reproducibility test of CS-GQDs based sensor.

undergoes further hydroxylation by dopamine β-hydroxylase (DBH) to form norepinephrine (NE), which is then methylated by phenylethanolamine N-methyltransferase (PNMT) to produce EP [90]. Thus, the structural characteristics of DA, including the primary amine group and its synthesis pathway, significantly enhance its interaction with the sensor surface, leading to the observed high selectivity for DA over potential interfering substances.

3.2. Repeatability, Reproducibility and Stability of CS-GQDs/Au Based Sensor

A sensor's repeatability is defined as its ability to yield the same findings in successive measurements while operating and ambient conditions are stable [91]. The repeatability of CS-GQDs/Au based sensor was evaluated by measuring the resonance angle shift following the injection of 1 fM of DA using the same sensor film as illustrated in Fig. 4. The observed peak likely resulted from the adsorption dynamics of DA molecules on the sensor surface. During repeated injections of DA at 1 fM concentration, slight variations in molecular interaction and surface coverage can occur, causing minor fluctuations in the resonance angle. The range of changes in $\Delta\theta$ observed on the y-axis is between 0.277° and 0.280°, which indicates that the variations are minimal and fall within a narrow range. This observation, combined with the calculated relative standard deviation (RSD) of 0.343%, highlights the remarkable precision and outstanding repeatability of this sensor, likely attributed to substantial DA adsorption on its surface.

The reproducibility of the sensor is an important performance criterion for its application [92]. So, the reproducibility of the proposed CS-GQDs based SPR sensor was also assessed by analyzing the response of six independent sensor films to 1 fM DA, as illustrated in Fig. 5. The calculated RSD value was 0.229%, indicating consistent and reliable performance of the sensor.

The sensor's stability was evaluated over a three-week period by exposing the sensor film to DA solution with the concentration of 1 fM and recording the sensor response. After one week, a minor increase in the angle shift was observed, from 0.2772° to 0.2778°. The resonance angle shift increased to 0.2789° after two weeks. The amount of angular shift was 0.2786° after three weeks as shown in Fig. 6. It was clearly seen that although the resonance angular shift decreased after the third week, it was still higher than the initial value, demonstrating excellent storage stability. These results indicate that the CS-GQDs based sensor demonstrates excellent repeatability, reproducibility, and durability over time, outperforms the two-week stability demonstrated by Jiang et al. [74] using conjugated polymer layers.

3.3. Real-Time Detection of DA with CS-GQDs/Au Based Sensor

The sensing process relies on the adsorption of DA molecules onto the CS-GQDs/Au surface, which induces a shift in the SPR angle. This shift is directly related to the concentration and adsorption kinetics of DA on the sensor surface. When a DA sample is introduced to the sensor, the DA molecules begin to bind to the CS-GQDs/Au film, leading to an increase in the refractive index at the sensor surface. This change is detected as a shift in the SPR dip, which is measured in real time. The kinetic behavior of the DA sample on the sensor film may be investigated by fitting the experimental findings to Pseudo-first-order (PFO) kinetic model represented as follows [93]:

$$\Delta\theta(t) = \Delta\theta_{eq}\left(1 - e^{-k_P t}\right) \quad (1)$$

where $\Delta\theta\,(t)$ signifies the resonance angular shift related to the adsorption of DA at time t; $\Delta\theta_{eq}$ represents the equilibrium resonance angular shift; and k_P is the adsorption rate constant.

The experimental findings for different concentrations of DA interacted with CS-GQDs/Au sensor film were fitted to PFO kinetic model to study the kinetic behaviour of DA on the surface of the sensor. Fig. 7 displays the shift in time of SPR dips

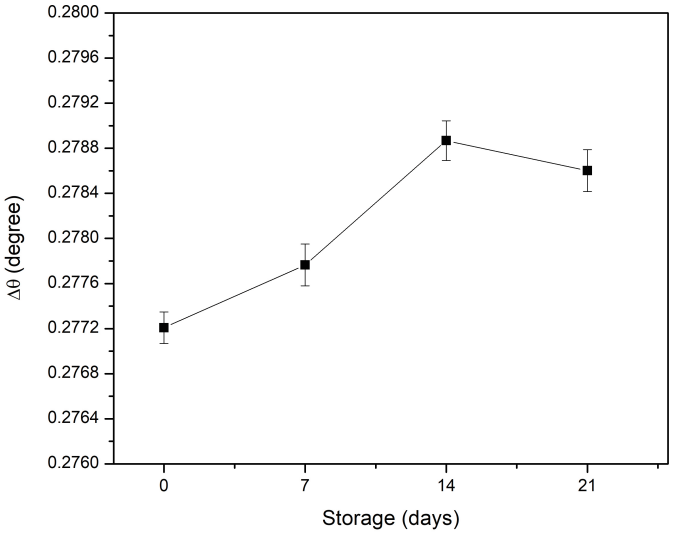

FIGURE 6. The stability evaluation of CS-GQDs based sensor.

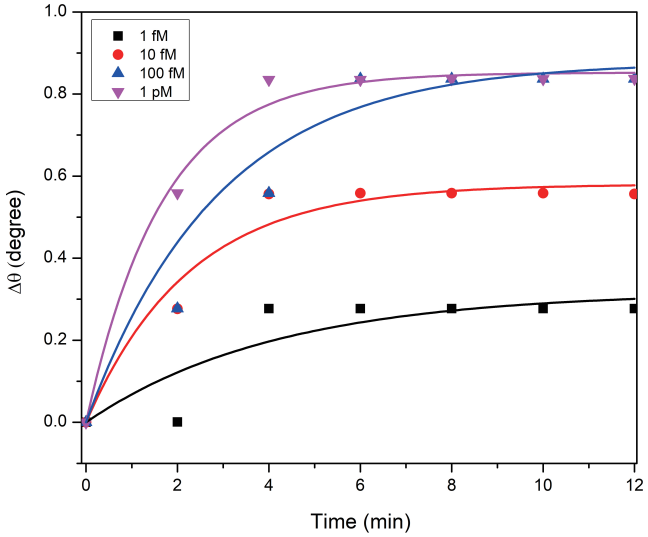

FIGURE 7. The sensorgram of DA adsorption on CS-GQDs/Au bilayer film in real-time.

throughout the first 12 minutes, encompassing the association phase and steady state before beginning the dissociation phase. During the interaction, the SPR dip initially shifted in response to the DA molecules binding to the sensor surface, reaching a steady state when adsorption is nearly complete. The equilibrium SPR shift increased with higher concentrations of DA, as more molecules interacted with the sensor surface. After reaching equilibrium, the sensor signals remained stable, reflecting the maximum binding capacity of the sensor surface for the given DA concentration. For 1 fM DA contacted the sensor film, the equilibrium SPR angular shift was 0.318°, and the adsorption rate constant was $0.240\ \text{min}^{-1}$. Next, for higher concentrations, the sensor response increased significantly as shown in Table 1. In case of 1 pM of DA, the fitting yielded the highest equilibrium SPR angular shift of 0.887° and adsorption rate constant of $0.712\ \text{min}^{-1}$ with R^2 of 0.976. The stable response signals were observed around 10 minutes after the injection of all DA concentrations. Therefore, SPR measurements were conducted 10 minutes post-injection for all concentrations to ensure complete interaction between DA and the CS-GQDs film.

TABLE 1. The kinetic parameters derived from PFO kinetic model for the adsorption of DA on CS-GQDs/Au bilayer film.

DA Concentration (fM)	$\Delta\theta_{eq}$ (degree)	k_P (min^{-1})	R^2
1	0.31	0.240	0.748
10	0.580	0.445	0.955
100	0.87	0.347	0.960
1000	0.88	0.712	0.976

3.4. Structural Characterization of CS-GQDs Film

To investigate the chemical structure and evidence, the functional groups exist in DA, and CS-GQDs nanocomposite before and after contacting with DA, and FTIR analysis was performed. The FTIR spectrum of DA shown in Fig. 8 revealed characteristic peaks at $3347\ \text{cm}^{-1}$ for amine N-H stretching, $1632\ \text{cm}^{-1}$ for amine N-H bending, $1523\ \text{cm}^{-1}$ for aromatic C = C stretching, and $1279\ \text{cm}^{-1}$ for amine C-N stretching [94].

In FTIR spectrum of CS-GQDs layer, the O–H bond stretching has been linked to the vibrational peaks at 3863 and $3740\ \text{cm}^{-1}$ as shown in Fig. 9. While the peak located at $3010\ \text{cm}^{-1}$ originates due to the stretching of C–H [95–100], the peaks found at 2783 and $2378\ \text{cm}^{-1}$ originate owing to the stretching of C = O [96, 101–104]. The available peak at $2139\ \text{cm}^{-1}$ is a result of the stretching vibrations of C ≡ C, whereas the peaks at 2004 and $1772\ \text{cm}^{-1}$ are attributed to the stretching vibrations of C = O [95, 105–108]. The band seen at $1706\ \text{cm}^{-1}$ region corresponds to the vibration of C = C stretching [109, 110]. The located peak near $1512\ \text{cm}^{-1}$ is due to imine bond — C = N produced because of the major amines of CS [111]. The peak located at $1342\ \text{cm}^{-1}$ is attributed to the C-H and N-H stretching vibration and the bending vibrations of C-N = bond [98, 103, 105, 112–114]. That peak at $1210\ \text{cm}^{-1}$ appeared as a result of C-O-C stretching, and the available peaks at 863, 702, and $587\ \text{cm}^{-1}$ are attributed to C-H bending [104, 105, 108, 110, 115]. The spectra of CS-GQDs/DA corroborated the loading of DA into the nanocomposite, since the peaks at 3863, 3740, 3010, and $1512\ \text{cm}^{-1}$ showed a reduction in their intensity attributed to overlap with the stretching vibrations of N-H bond. Conversely, the peaks around 2090, 1342, and $1199\ \text{cm}^{-1}$ showed enhanced intensity, corresponding to the stretching vibrations of C-N. The new peak emerged at $618\ \text{cm}^{-1}$ attributed to the amine C-N stretching [98, 102, 116, 117]. These results show that CS-GQDs nanocomposite film was effectively deposited on the gold surface and confirm that DA binding occurred on the sensor surface, altering its refractive index.

The surface morphology of CS-GQDs/Au bilayer film, prior to and following the interaction with DA with scanning size of $1\ \mu\text{m} \times 1\ \mu\text{m}$ is shown in Fig. 10(a) and Fig. 10(b), respectively. The three-dimensional (3D) AFM image (Fig. 10(c)) of

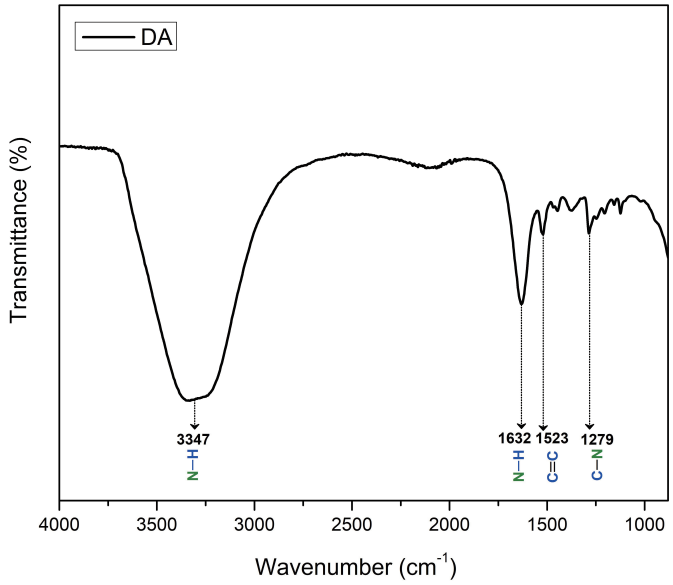

FIGURE 8. FTIR spectrum of DA solution.

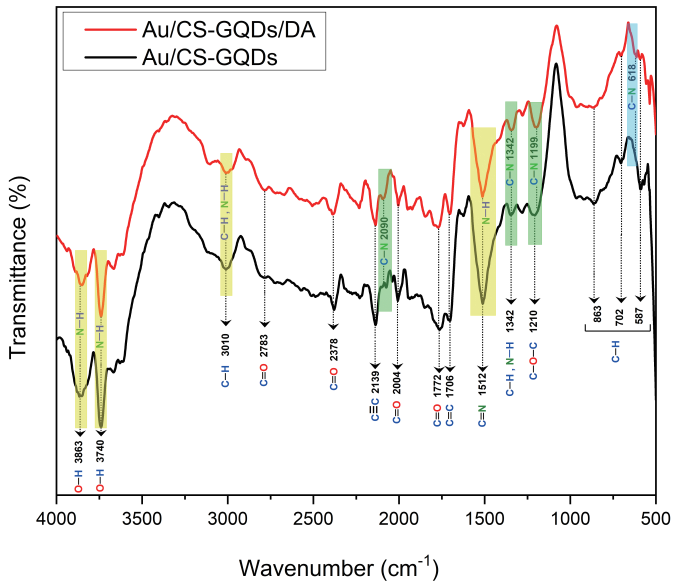

FIGURE 9. FTIR spectrum of CS-GQDs nanocomposite prior to and after interaction with DA solution (the transmission level with DA was intensionally increased by a constant for easy comparisson with that without DA).

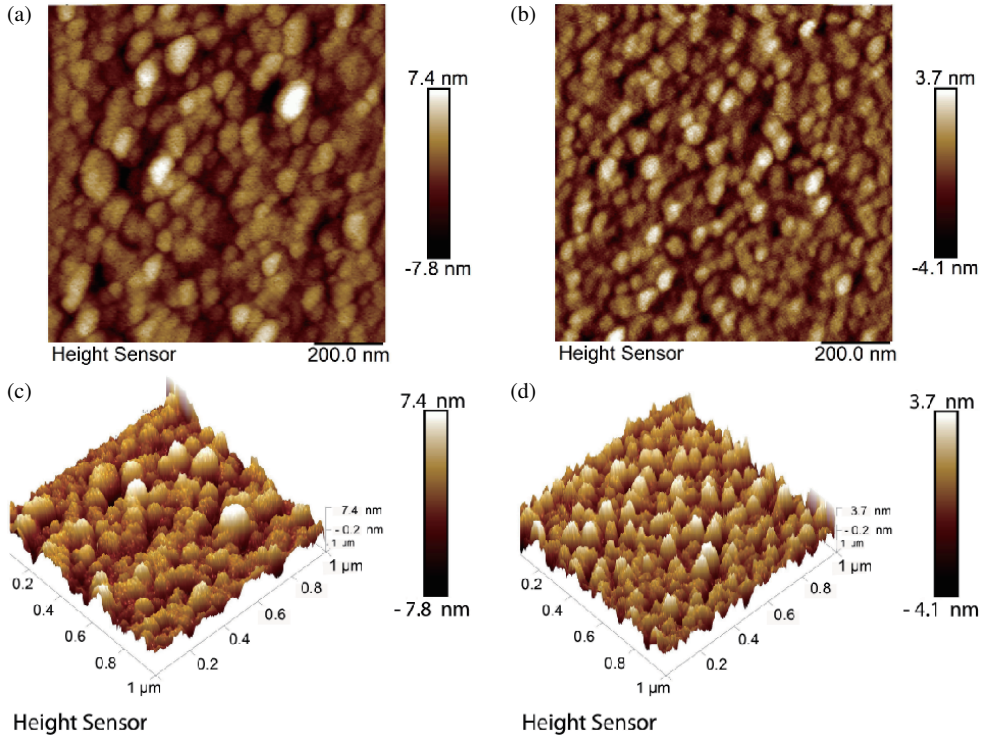

FIGURE 10. AFM-based analysis of CS-GQDs nanocomposite: (a) The 2D image prior to contact with DA sample; (b) The 2D image following contact with DA sample; (c) The 3D image prior to contact with DA sample; and (d) The 3D image following contact with DA sample.

CS-GQDs nanocomposite in the absence of DA showed some broad, divergent peaks of varying heights. Interestingly, the adsorbed DA molecules on the sensor film clearly affected its surface morphology, as seen in Fig. 10(b). The peaks became denser, sharper, shorter, and more uniformly distributed compared with the peaks before DA injection (Fig. 10(d), with a concentration of 1 fM DA). The average roughness Ra of the nanocomposite film changed from 1.610 to 0.900 nm when DA solution was introduced to the sensing system, and Rq decreased from 2.080 to 1.130 nm. The obtained results show that DA binding to the CS-GQDs nanocomposite film happened and significantly impacted its morphology.

4. CONCLUSIONS

To conclude, in this study we conducted a thorough analysis of the sensing performance of the proposed sensor toward the clinically significant neurotransmitter DA. The sensor's ability to detect DA in the presence of other potentially competitive interfering samples was evaluated. The results revealed the sensor potential to detect extremely low levels of DA solution (1 pM) even in the presence of higher concentrations of EP, UA, and AA. Furthermore, the results demonstrated outstanding repeatability and reproducibility of the sensor with RSD values of 0.343% and 0.229%, respectively, as well as long-term stability. By fitting the experimental data to the PFO kinetic model, the kinetic behavior of DA molecules on the sensor surface was also investigated. Real-time DA detection demonstrated that the obtained response signals were stable after roughly 10 minutes of DA injection at all concentrations. The adsorption of DA to the CS-GQDs/Au sensor film was validated through the structural investigation of the sensing film, which revealed changes in the spectral bands and peak intensities of FTIR spectra, as well as alterations in the sensor film's surface morphology and roughness. The benefits of this sensor's sensitivity, selectivity, stability, and efficiency in real-time target detection, as well as other detecting features, make it superior and preferable to other sensors.

AUTHOR CONTRIBUTIONS

Conceptualization, Y. W. Fen and F. B. Kamal Eddin; methodology, writing — original draft preparation, F. B. Kamal Eddin; supervision, validation, funding acquisition, Y. W. Fen; writing — review and editing, Y. W. Fen; H. N. Lim, K. Cui, S. Hou and F. B. Kamal Eddin; resources, Y. W. Fen, J. Y. C. Liew, N. I. M. Fauzi and W. M. E. M. M. Daniyal; software, F. B. Kamal Eddin; visualization, F. B. Kamal Eddin. All authors have read and agreed to the published version of the manuscript.

FUNDING

This research was funded by the Ministry of Education Malaysia through the Fundamental FRGS (FRGS/1/2019/STG02/UPM/02/1) and Universiti Putra Malaysia through Putra Grant (GP-IPB/2021/9700700), Zhejiang Provincial Basic and Public Welfare Research Program (NO: LGC20H090001), and "Pioneer" and "Leading Goose" R&D Program of Zhejiang Province (2023C03083).

ACKNOWLEDGEMENT

F. B. Kamal Eddin gratefully acknowledges the support received from OWSD and Sida (Swedish International Development Cooperation Agency), the laboratory facilities provided by the Institute of Nanoscience and Nanotechnology, Department of Physics, Department of Chemistry, Universiti Putra Malaysia.

DECLARATION OF COMPETING INTEREST

The authors declare that they have no known competing financial interests or personal relationships that could have appeared to influence the work reported in this paper.

DATA AVAILABILITY

All data required to reproduce these findings are included into the paper.

REFERENCES

[1] Gupta, B. D., A. Pathak, and V. Semwal, "Carbon-based nanomaterials for plasmonic sensors: A review," *Sensors*, Vol. 19, No. 16, 3536, 2019.

[2] Situ, C., M. H. Mooney, C. T. Elliott, and J. Buijs, "Advances in surface plasmon resonance biosensor technology towards high-throughput, food-safety analysis," *TrAC Trends in Analytical Chemistry*, Vol. 29, No. 11, 1305–1315, 2010.

[3] Soler, M., C. S. Huertas, and L. M. Lechuga, "Label-free plasmonic biosensors for point-of-care diagnostics: A review," *Expert Review of Molecular Diagnostics*, Vol. 19, No. 1, 71–81, 2019.

[4] Semwal, V. and B. D. Gupta, "Highly sensitive surface plasmon resonance based fiber optic pH sensor utilizing rGO-Pani nanocomposite prepared by in situ method," *Sensors and Actuators B: Chemical*, Vol. 283, 632–642, 2019.

[5] Omar, N. A. S., Y. W. Fen, J. Abdullah, Y. M. Kamil, W. M. E. M. M. Daniyal, A. R. Sadrolhosseini, and M. A. Mahdi, "Sensitive detection of dengue virus type 2 E-Proteins signals using self-assembled monolayers/reduced graphene oxide-PAMAM Dendrimer thin film-SPR Optical sensor," *Scientific Reports*, Vol. 10, No. 1, 2374, 2020.

[6] Bocková, M., X. C. Song, E. Gedeonová, K. Levová, M. Kalousová, T. Zima, and J. Homola, "Surface plasmon resonance biosensor for detection of pregnancy associated plasma protein A2 in clinical samples," *Analytical and Bioanalytical Chemistry*, Vol. 408, 7265–7269, 2016.

[7] Yang, W., Y.-F. C. Chau, and S.-C. Jheng, "Analysis of transmittance properties of surface plasmon modes on periodic solid/outline bowtie nanoantenna arrays," *Physics of Plasmas*, Vol. 20, No. 6, 064503, 2013.

[8] Chao, C.-T. C., M. R. R. Kooh, Y.-F. C. Chau, and R. Thotagamuge, "Susceptible plasmonic photonic crystal fiber sensor with elliptical air holes and external-flat gold-coated surface," in *Photonics*, Vol. 9, No. 12, 916, 2022.

[9] Chao, C.-T. C., Y.-F. C. Chau, and H.-P. Chiang, "Multiple Fano resonance modes in an ultra-compact plasmonic waveguide-cavity system for sensing applications," *Results in Physics*, Vol. 27, 104527, 2021.

[10] Chao, C.-T. C., M. U. Ahmed, H. J. Huang, C. M. Lim, M. R. R. Kooh, R. Thotagamuge, and Y.-F. C. Chau, "A simple structure of high sensitivity of plasmonic photonic crystal fiber sensors with minimal air hole density in fiber cladding," *Plasmonics*, 1–12, 2024.

[11] Kim, H.-M., J.-H. Park, and S.-K. Lee, "Fabrication and measurement of a fiber optic localized surface plasmon resonance sensor chip for molecular diagnostics," *Sensors and Actuators A: Physical*, Vol. 331, 112982, 2021.

[12] Jeon, J., S. Uthaman, J. Lee, H. Hwang, G. Kim, P. J. Yoo, B. D. Hammock, C. S. Kim, Y.-S. Park, and I.-K. Park, "In-direct localized surface plasmon resonance (LSPR)-based nanosensors

for highly sensitive and rapid detection of cortisol," *Sensors and Actuators B: Chemical*, Vol. 266, 710–716, 2018.

[13] Chau, Y.-F. and Z.-H. Jiang, "Plasmonics effects of nanometal embedded in a dielectric substrate," *Plasmonics*, Vol. 6, 581–589, 2011.

[14] Cui, X., J. Li, Y. Li, M. Liu, J. Qiao, D. Wang, H. Cao, W. He, Y. Feng, and Z. Yang, "Detection of glucose in diabetic tears by using gold nanoparticles and MXene composite surface-enhanced Raman scattering substrates," *Spectrochimica Acta Part A: Molecular and Biomolecular Spectroscopy*, Vol. 266, 120432, 2022.

[15] Guo, J., Y. Liu, H. Ju, and G. Lu, "From lab to field: Surface-enhanced Raman scattering-based sensing strategies for on-site analysis," *TrAC Trends in Analytical Chemistry*, Vol. 146, 116488, 2022.

[16] Enders, D., S. Rupp, A. Küller, and A. Pucci, "Surface enhanced infrared absorption on Au nanoparticle films deposited on SiO_2/Si for optical biosensing: Detection of the antibody-antigen reaction," *Surface Science*, Vol. 600, No. 23, L305–L308, 2006.

[17] Janneh, M., "Surface enhanced infrared absorption spectroscopy using plasmonic nanostructures: Alternative ultrasensitive on-chip biosensor technique," *Results in Optics*, Vol. 6, 100201, 2022.

[18] Peixoto, L. P. F., J. F. L. Santos, and G. F. S. Andrade, "Surface enhanced fluorescence immuno-biosensor based on gold nanorods," *Spectrochimica Acta Part A: Molecular and Biomolecular Spectroscopy*, Vol. 284, 121753, 2023.

[19] Sultangaziyev, A. and R. Bukasov, "Applications of surface-enhanced fluorescence (SEF) spectroscopy in bio-detection and biosensing," *Sensing and Bio-Sensing Research*, Vol. 30, 100382, 2020.

[20] Fen, Y. W., W. M. M. Yunus, N. A. Yusof, N. S. Ishak, N. A. S. Omar, and A. A. Zainudin, "Preparation, characterization and optical properties of ionophore doped chitosan biopolymer thin film and its potential application for sensing metal ion," *Optik*, Vol. 126, No. 23, 4688–4692, 2015.

[21] Daniyal, W. M. E. M. M., Y. W. Fen, J. Abdullah, A. R. Sadrolhosseini, and M. A. Mahdi, "Design and optimization of surface plasmon resonance spectroscopy for optical constant characterization and potential sensing application: Theoretical and experimental approaches," in *Photonics*, Vol. 8, No. 9, 361, 2021.

[22] Daniyal, W. M. E. M. M., Y. W. Fen, F. B. Kamal Eddin, J. Abdullah, and M. A. Mahdi, "Surface plasmon resonance assisted optical characterization of nickel ion solution and nanocrystalline cellulose-graphene oxide thin film for sensitivity enhancement analysis," *Physica B: Condensed Matter*, Vol. 646, 414292, 2022.

[23] Fen, Y. W., W. M. M. Yunus, and Z. A. Talib, "Analysis of Pb (II) ion sensing by crosslinked chitosan thin film using surface plasmon resonance spectroscopy," *Optik*, Vol. 124, No. 2, 126–133, 2013.

[24] Fen, Y. W., W. Yunus, and N. A. Yusof, "Optical properties of cross-linked chitosan thin film for copper ion detection using surface plasmon resonance technique," *Optica Applicata*, Vol. 41, No. 4, 999–1013, 2011.

[25] Sadeghi, Z., T. Hajiani, and H. Shirkani, "Optical properties of anisotropic phosphorene-graphene nanotubes and their application as label-free SPR biosensors in IR," *Materials Science and Engineering: B*, Vol. 278, 115615, 2022.

[26] Daniyal, M., W. M. E. Mustaqim, S. Saleviter, and Y. W. Fen, "Development of surface plasmon resonance spectroscopy for metal ion detection," *Sensors & Materials*, Vol. 30, No. 9, 2023–2038, 2018.

[27] Fauzi, N. I. M., Y. W. Fen, N. A. S. Omar, S. Saleviter, W. M. E. M. M. Daniyal, H. S. Hashim, and M. Nasrullah, "Nanostructured chitosan/maghemite composites thin film for potential optical detection of mercury ion by surface plasmon resonance investigation," *Polymers*, Vol. 12, No. 7, 1497, 2020.

[28] Omar, N. A. S., R. Irmawati, Y. W. Fen, E. N. Muhamad, F. B. Kamal Eddin, N. A. A. Anas, N. S. M. Ramdzan, N. I. M. Fauzi, and M. A. Mahdi, "Surface refractive index sensor based on titanium dioxide composite thin film for detection of cadmium ions," *Measurement*, Vol. 187, 110287, 2022.

[29] Xia, G., C. Zhou, S. Jin, C. Huang, J. Xing, and Z. Liu, "Sensitivity enhancement of two-dimensional materials based on genetic optimization in surface plasmon resonance," *Sensors*, Vol. 19, No. 5, 1198, 2019.

[30] Fen, Y. W., W. M. M. Yunus, and N. A. Yusof, "Surface plasmon resonance optical sensor for detection of Pb^{2+} based on immobilized p-tert-butylcalix [4] arene-tetrakis in chitosan thin film as an active layer," *Sensors and Actuators B: Chemical*, Vol. 171, 287–293, 2012.

[31] Cairns, T. M., N. T. Ditto, D. Atanasiu, H. Lou, B. D. Brooks, W. T. Saw, R. J. Eisenberg, and G. H. Cohen, "Surface plasmon resonance reveals direct binding of herpes simplex virus glycoproteins gH/gL to gD and locates a gH/gL binding site on gD," *Journal of Virology*, Vol. 93, No. 15, e00 289–19, 2019.

[32] Fen, Y. W., W. M. M. Yunus, Z. A. Talib, and N. A. Yusof, "Development of surface plasmon resonance sensor for determining zinc ion using novel active nanolayers as probe," *Spectrochimica Acta Part A: Molecular and Biomolecular Spectroscopy*, Vol. 134, 48–52, 2015.

[33] Sarcina, L., G. F. Mangiatordi, F. Torricelli, P. Bollella, Z. Gounani, R. Österbacka, E. Macchia, and L. Torsi, "Surface plasmon resonance assay for label-free and selective detection of HIV-1 p24 protein," *Biosensors*, Vol. 11, No. 6, 180, 2021.

[34] Jang, D., G. Chae, and S. Shin, "Analysis of surface plasmon resonance curves with a novel sigmoid-asymmetric fitting algorithm," *Sensors*, Vol. 15, No. 10, 25 385–25 398, 2015.

[35] Puiu, M. and C. Bala, "SPR and SPR imaging: Recent trends in developing nanodevices for detection and real-time monitoring of biomolecular events," *Sensors*, Vol. 16, No. 6, 870, 2016.

[36] Sharma, S. and B. D. Gupta, "Surface plasmon resonance based highly selective fiber optic dopamine sensor fabricated using molecular imprinted GNP/SnO_2 nanocomposite," *Journal of Lightwave Technology*, Vol. 36, No. 24, 5956–5962, 2018.

[37] Do, M. H., B. Dubreuil, J. Peydecastaing, G. Vaca-Medina, T.-T. Nhu-Trang, N. Jaffrezic-Renault, and P. Behra, "Chitosan-based nanocomposites for glyphosate detection using surface plasmon resonance sensor," *Sensors*, Vol. 20, No. 20, 5942, 2020.

[38] Szunerits, S., J. Spadavecchia, and R. Boukherroub, "Surface plasmon resonance: Signal amplification using colloidal gold nanoparticles for enhanced sensitivity," *Reviews in Analytical Chemistry*, Vol. 33, No. 3, 153–164, 2014.

[39] Wang, Q., Q. Li, X. Yang, K. Wang, S. Du, H. Zhang, and Y. Nie, "Graphene oxide-gold nanoparticles hybrids-based surface plasmon resonance for sensitive detection of microRNA," *Biosensors and Bioelectronics*, Vol. 77, 1001–1007, 2016.

[40] Luan, Q., K. Zhou, H. Tan, D. Yang, and X. Yao, "Au-NPs enhanced SPR biosensor based on hairpin DNA without the effect of nonspecific adsorption," *Biosensors and Bioelectronics*, Vol. 26, No. 5, 2473–2477, 2011.

[41] Takahata, R., S. Yamazoe, K. Koyasu, and T. Tsukuda, "Surface plasmon resonance in gold ultrathin nanorods and nanowires,"

Journal of the American Chemical Society, Vol. 136, No. 24, 8489–8491, 2014.

[42] Tabasi, O. and C. Falamaki, "Recent advancements in the methodologies applied for the sensitivity enhancement of surface plasmon resonance sensors," *Analytical Methods*, Vol. 10, No. 32, 3906–3925, 2018.

[43] Wang, M., Y. Huo, S. Jiang, C. Zhang, C. Yang, T. Ning, X. Liu, C. Li, W. Zhang, and B. Man, "Theoretical design of a surface plasmon resonance sensor with high sensitivity and high resolution based on graphene-WS2 hybrid nanostructures and Au-Ag bimetallic film," *RSC Advances*, Vol. 7, No. 75, 47 177–47 182, 2017.

[44] Chen, S. and C. Lin, "High-performance bimetallic film surface plasmon resonance sensor based on film thickness optimization," *Optik*, Vol. 127, No. 19, 7514–7519, 2016.

[45] Fauzi, N. I. M., Y. W. Fen, F. B. Kamal Eddin, and W. M. E. M. M. Daniyal, "Structural and optical properties of graphene quantum dots-polyvinyl alcohol composite thin film and its potential in plasmonic sensing of carbaryl," *Nanomaterials*, Vol. 12, No. 22, 4105, 2022.

[46] Chen, J.-L., X.-P. Yan, K. Meng, and S.-F. Wang, "Graphene oxide based photoinduced charge transfer label-free near-infrared fluorescent biosensor for dopamine," *Analytical Chemistry*, Vol. 83, No. 22, 8787–8793, 2011.

[47] Haque, T. and H. K. Rouf, "DNA hybridization detection using graphene-MoSe2-Ag heterostructure-based surface plasmon resonance biosensor," *Applied Physics A*, Vol. 127, No. 10, 759, 2021.

[48] Fauzi, N. I. M., Y. W. Fen, J. Abdullah, M. A. Kamarudin, N. A. S. Omar, F. B. Kamal Eddin, N. S. M. Ramdzan, and W. M. E. M. M. Daniyal, "Evaluation of structural and optical properties of graphene oxide-polyvinyl alcohol thin film and its potential for pesticide detection using an optical method," in *Photonics*, Vol. 9, No. 5, 300, 2022.

[49] Zainudin, A. A., Y. W. Fen, N. A. Yusof, S. H. Al-Rekabi, M. A. Mahdi, and N. A. S. Omar, "Incorporation of surface plasmon resonance with novel valinomycin doped chitosan-graphene oxide thin film for sensing potassium ion," *Spectrochimica Acta Part A: Molecular and Biomolecular Spectroscopy*, Vol. 191, 111–115, 2018.

[50] Bhavsar, K. and R. Prabhu, "Investigations on sensitivity enhancement of SPR biosensor using tunable wavelength and graphene layers," in *IOP Conference Series: Materials Science and Engineering*, Vol. 499, No. 1, 012008, 2019.

[51] Hashim, H. S., Y. W. Fen, N. A. S. Omar, J. Abdullah, W. M. E. M. M. Daniyal, and S. Saleviter, "Detection of phenol by incorporation of gold modified-enzyme based graphene oxide thin film with surface plasmon resonance technique," *Optics Express*, Vol. 28, No. 7, 9738–9752, 2020.

[52] Anas, N. A. A., Y. W. Fen, N. A. S. Omar, N. S. M. Ramdzan, W. M. E. M. M. Daniyal, S. Saleviter, and A. A. Zainudin, "Optical properties of chitosan/hydroxyl-functionalized graphene quantum dots thin film for potential optical detection of ferric (III) ion," *Optics & Laser Technology*, Vol. 120, 105724, 2019.

[53] Çimen, D., S. Aslıyüc, T. D. Tanalp, and A. Denizli, "Molecularly imprinted nanofilms for endotoxin detection using an surface plasmon resonance sensor," *Analytical Biochemistry*, Vol. 632, 114221, 2021.

[54] Puttharugsa, C., T. Wangkam, N. Houngkamhang, S. Yodmongkol, O. Gajanandana, O. Himananto, B. Sutapun, R. Amarit, A. Somboonkaew, and T. Srikhirin, "A polymer surface for antibody detection by using surface plasmon resonance via immobilized antigen," *Current Applied Physics*, Vol. 13, No. 6, 1008–1013, 2013.

[55] Nurrohman, D. T. and N.-F. Chiu, "A review of graphene-based surface plasmon resonance and surface-enhanced raman scattering biosensors: Current status and future prospects," *Nanomaterials*, Vol. 11, No. 1, 216, 2021.

[56] Arulraj, A. D., A. Arunkumar, M. Vijayan, K. B. Viswanath, and V. S. Vasantha, "A simple route to develop highly porous nano polypyrrole/reduced graphene oxide composite film for selective determination of dopamine," *Electrochimica Acta*, Vol. 206, 77–85, 2016.

[57] Li, Y., H. Song, L. Zhang, P. Zuo, B.-C. Ye, J. Yao, and W. Chen, "Supportless electrochemical sensor based on molecularly imprinted polymer modified nanoporous microrod for determination of dopamine at trace level," *Biosensors and Bioelectronics*, Vol. 78, 308–314, 2016.

[58] Krishna, V. M., T. Somanathan, E. Manikandan, K. K. Tadi, and S. Uvarajan, "Neurotransmitter dopamine enhanced sensing detection using fibre-like carbon nanotubes by chemical vapor deposition technique," *Journal of Nanoscience and Nanotechnology*, Vol. 18, No. 8, 5380–5389, 2018.

[59] Kunpatee, K., S. Traipop, O. Chailapakul, and S. Chuanuwatanakul, "Simultaneous determination of ascorbic acid, dopamine, and uric acid using graphene quantum dots/ionic liquid modified screen-printed carbon electrode," *Sensors and Actuators B: Chemical*, Vol. 314, 128059, 2020.

[60] Yusoff, N., A. Pandikumar, R. Ramaraj, H. N. Lim, and N. M. Huang, "Gold nanoparticle based optical and electrochemical sensing of dopamine," *Microchimica Acta*, Vol. 182, 2091–2114, 2015.

[61] Kujawska, M., S. K. Bhardwaj, Y. K. Mishra, and A. Kaushik, "Using graphene-based biosensors to detect dopamine for efficient parkinson's disease diagnostics," *Biosensors*, Vol. 11, No. 11, 433, 2021.

[62] Sun, X., L. Zhang, X. Zhang, X. Liu, J. Jian, D. Kong, D. Zeng, H. Yuan, and S. Feng, "Electrochemical dopamine sensor based on superionic conducting potassium ferrite," *Biosensors and Bioelectronics*, Vol. 153, 112045, 2020.

[63] Cai, L., B. Hou, Y. Shang, L. Xu, B. Zhou, X. Jiang, and X. Jiang, "Synthesis of fe_3o_4/graphene oxide/pristine graphene ternary composite and fabrication electrochemical sensor to detect dopamine and hydrogen peroxide," *Chemical Physics Letters*, Vol. 736, 136797, 2019.

[64] Sarno, M., S. Galvagno, C. Scudieri, P. Iovane, S. Portofino, C. Borriello, and C. Cirillo, "Dopamine sensor in real sample based on thermal plasma silicon carbide nanopowders," *Journal of Physics and Chemistry of Solids*, Vol. 131, 213–222, 2019.

[65] Kokulnathan, T., T.-J. Wang, E. A. Kumar, N. Duraisamy, and A.-T. Lee, "An electrochemical platform based on yttrium oxide/boron nitride nanocomposite for the detection of dopamine," *Sensors and Actuators B: Chemical*, Vol. 349, 130787, 2021.

[66] Sansuk, S., E. Bitziou, M. B. Joseph, J. A. Covington, M. G. Boutelle, P. R. Unwin, and J. V. Macpherson, "Ultrasensitive detection of dopamine using a carbon nanotube network microfluidic flow electrode," *Analytical Chemistry*, Vol. 85, No. 1, 163–169, 2013.

[67] Prasad, B. B., D. Jauhari, and M. P. Tiwari, "A dual-template imprinted polymer-modified carbon ceramic electrode for ultra trace simultaneous analysis of ascorbic acid and dopamine," *Biosensors and Bioelectronics*, Vol. 50, 19–27, 2013.

[68] Yin, T., W. Wei, and J. Zeng, "Selective detection of dopamine in the presence of ascorbic acid by use of glassy-carbon elec-

trodes modified with both polyaniline film and multi-walled carbon nanotubes with incorporated β-cyclodextrin," *Analytical and Bioanalytical Chemistry*, Vol. 386, 2087–2094, 2006.

[69] Ye, N. and J. Li, "Determination of dopamine, epinephrine, and norepinephrine by open-tubular capillary electrochromatography using graphene oxide molecularly imprinted polymers as the stationary phase," *Journal of Separation Science*, Vol. 37, No. 16, 2239–2247, 2014.

[70] Wang, C., R. Yuan, Y. Chai, Y. Zhang, F. Hu, and M. Zhang, "Au-nanoclusters incorporated 3-amino-5-mercapto-1, 2, 4-triazole film modified electrode for the simultaneous determination of ascorbic acid, dopamine, uric acid and nitrite," *Biosensors and Bioelectronics*, Vol. 30, No. 1, 315–319, 2011.

[71] Dutta, P., R. B. Pernites, C. Danda, and R. C. Advincula, "SPR detection of dopamine using cathodically electropolymerized, molecularly imprinted poly-p-aminostyrene thin films," *Macromolecular Chemistry and Physics*, Vol. 212, No. 22, 2439–2451, 2011.

[72] Kamali, K. Z., A. Pandikumar, G. Sivaraman, H. N. Lim, S. P. Wren, T. Sun, and N. M. Huang, "Silver@ graphene oxide nanocomposite-based optical sensor platform for biomolecules," *RSC Advances*, Vol. 5, No. 23, 17 809–17 816, 2015.

[73] Raj, D. R., S. Prasanth, T. V. Vineeshkumar, and C. Sudarsanakumar, "Surface plasmon resonance based fiber optic dopamine sensor using green synthesized silver nanoparticles," *Sensors and Actuators B: Chemical*, Vol. 224, 600–606, 2016.

[74] Jiang, K., Y. Wang, G. Thakur, Y. Kotsuchibashi, S. Naicker, R. Narain, and T. Thundat, "Rapid and highly sensitive detection of dopamine using conjugated oxaborole-based polymer and glycopolymer systems," *ACS Applied Materials & Interfaces*, Vol. 9, No. 18, 15 225–15 231, 2017.

[75] Manaf, A. a., M. Ghadiry, R. Soltanian, H. Ahmad, and C. K. Lai, "Picomole dopamine detection using optical chips," *Plasmonics*, Vol. 12, 1505–1510, 2017.

[76] Jabbari, S., B. Dabirmanesh, S. Daneshjou, and K. Khajeh, "The potential of a novel enzyme-based surface plasmon resonance biosensor for direct detection of dopamine," *Scientific Reports*, Vol. 14, No. 1, 14303, 2024.

[77] Wekalao, J. and N. Mandela, "Graphene metasurface-based biosensor for direct dopamine detection utilizing surface plasmon resonance in the terahertz regime with machine learning optimization via K-nearest neighbors regression," *Plasmonics*, 1–29, 2024.

[78] Karki, B., Y. Trabelsi, A. Pal, S. A. Taya, and R. B. Yadav, "Direct detection of dopamine using zinc oxide nanowire-based surface plasmon resonance sensor," *Optical Materials*, Vol. 147, 114555, 2024.

[79] Sharma, P. S., K. Choudhary, and S. Kumar, "High-fidelity dopamine detection with 2-D material-assisted and plasmon-enhanced etched core-mismatched optical fiber sensor," *IEEE Transactions on Plasma Science*, Vol. 52, No. 7, 2818–2825, 2024.

[80] Huang, Y., X. Li, H. Zhang, Z. Wu, R. Weerasooriya, X. Chen, J. Zhou, J. Wu, J. Xue, J. Wang, and L. Feng, "Development of an optical fiber surface plasmon resonance sensor decorated with MoS2/AuNP plasmonic hybrid structure by using polydopamine-assisted electroless plating," *Optics & Laser Technology*, Vol. 183, 112255, 2025.

[81] Kamal Eddin, F. B., Y. W. Fen, N. A. S. Omar, J. Y. C. Liew, and W. M. E. M. M. Daniyal, "Femtomolar detection of dopamine using surface plasmon resonance sensor based on chitosan/graphene quantum dots thin film," *Spectrochimica Acta Part A: Molecular and Biomolecular Spectroscopy*, Vol. 263, 120202, 2021.

[82] Kamal Eddin, F. B. and Y. W. Fen, "The principle of nanomaterials based surface plasmon resonance biosensors and its potential for dopamine detection," *Molecules*, Vol. 25, No. 12, 2769, 2020.

[83] Kamal Eddin, F. B., Y. W. Fen, J. Y. C. Liew, H. N. Lim, W. M. E. M. M. Daniyal, and N. A. S. Omar, "Simultaneous measurement of the refractive index and thickness of graphene oxide/gold multilayered structure for potential in dopamine sensing using surface plasmon resonance spectroscopy," *Optik*, Vol. 278, 170703, 2023.

[84] Kamal Eddin, F. B., Y. W. Fen, N. I. M. Fauzi, W. M. E. M. M. Daniyal, N. A. S. Omar, M. F. Anuar, H. S. Hashim, A. R. Sadrolhosseini, and H. Abdullah, "Direct and sensitive detection of dopamine using carbon quantum dots based refractive index surface plasmon resonance sensor," *Nanomaterials*, Vol. 12, No. 11, 1799, 2022.

[85] Kamal Eddin, F. B., Y. W. Fen, J. Y. C. Liew, and W. M. E. M. M. Daniyal, "Plasmonic refractive index sensor enhanced with chitosan/Au bilayer thin film for dopamine detection," *Biosensors*, Vol. 12, No. 12, 1124, 2022.

[86] Kamal Eddin, F. B., Y. W. Fen, J. Y. C. Liew, H. N. Lim, N. I. M. Fauzi, and W. M. E. M. M. Daniyal, "Structural, optical and plasmonic sensing characteristics of graphene quantum dots/gold nanolayered film in contact with dopamine solution," *Optical and Quantum Electronics*, Vol. 55, No. 14, 1222, 2023.

[87] Kamal Eddin, F. B., Y. W. Fen, A. R. Sadrolhosseini, J. Y. C. Liew, and W. M. E. M. M. Daniyal, "Optical property analysis of chitosan-graphene quantum dots thin film and dopamine using surface plasmon resonance spectroscopy," *Plasmonics*, Vol. 17, No. 5, 1985–1997, 2022.

[88] Chao, C.-T. C., S.-H. Chen, H. J. Huang, M. R. R. Kooh, C. M. Lim, R. Thotagamuge, A. H. Mahadi, and Y.-F. C. Chau, "Improving temperature-sensing performance of photonic crystal fiber via external metal-coated trapezoidal-shaped surface," *Crystals*, Vol. 13, No. 5, 813, 2023.

[89] Chao, C.-T. C., M. R. R. Kooh, C. M. Lim, R. Thotagamuge, A. H. Mahadi, and Y.-F. C. Chau, "Visible-range multiple-channel metal-shell rod-shaped narrowband plasmonic metamaterial absorber for refractive index and temperature sensing," *Micromachines*, Vol. 14, No. 2, 340, 2023.

[90] Hidalgo-Acosta, J. C., A. M. Jaramillo, and M. T. Cortés, "Distinguishing catecholamines: Dopamine determination in the presence of epinephrine in water/acetonitrile mixtures," *Electrochimica Acta*, Vol. 359, 136932, 2020.

[91] Meyyappan, M., "Carbon nanotube-based chemical sensors," *Small*, Vol. 12, No. 16, 2118–2129, 2016.

[92] Zonta, G., M. Astolfi, D. Casotti, G. Cruciani, B. Fabbri, A. Gaiardo, S. Gherardi, V. Guidi, N. Landini, M. Valt, and C. Malagù, "Reproducibility tests with zinc oxide thick-film sensors," *Ceramics International*, Vol. 46, No. 5, 6847–6855, 2020.

[93] Xu, H., B. Wang, R. Zhao, X. Wang, C. Pan, Y. Jiang, X. Zhang, and B. Ge, "Adsorption behavior and performance of ammonium onto sorghum straw biochar from water," *Scientific Reports*, Vol. 12, No. 1, 5358, 2022.

[94] Thakur, A., S. Ranote, D. Kumar, K. K. Bhardwaj, R. Gupta, and G. S. Chauhan, "Synthesis of a PEGylated dopamine ester with enhanced antibacterial and antifungal activity," *ACS Omega*, Vol. 3, No. 7, 7925–7933, 2018.

[95] Vijayalakshmi, K., B. M. Devi, P. N. Sudha, J. Venkatesan, and S. Anil, "Synthesis, characterization and applications of

nanochitosan/sodium alginate/microcrystalline cellulose film," *Journal of Nanomedicine & Nanotechnology*, Vol. 7, No. 419, 2, 2016.

[96] Teymourinia, H., M. Salavati-Niasari, O. Amiri, and H. Safardoust-Hojaghan, "Synthesis of graphene quantum dots from corn powder and their application in reduce charge recombination and increase free charge carriers," *Journal of Molecular Liquids*, Vol. 242, 447–455, 2017.

[97] Essel, T. Y. A., A. Koomson, M.-P. O. Seniagya, G. P. Cobbold, S. K. Kwofie, B. O. Asimeng, P. K. Arthur, G. Awandare, and E. K. Tiburu, "Chitosan composites synthesized using acetic acid and tetraethylorthosilicate respond differently to methylene blue adsorption," *Polymers*, Vol. 10, No. 5, 466, 2018.

[98] Abazar, F. and A. Noorbakhsh, "Chitosan-carbon quantum dots as a new platform for highly sensitive insulin impedimetric aptasensor," *Sensors and Actuators B: Chemical*, Vol. 304, 127281, 2020.

[99] Choppadandi, M., A. T. Guduru, P. Gondaliya, N. Arya, K. Kalia, H. Kumar, and G. Kapusetti, "Structural features regulated photoluminescence intensity and cell internalization of carbon and graphene quantum dots for bioimaging," *Materials Science and Engineering: C*, Vol. 129, 112366, 2021.

[100] Zam, Z. Z., F. Muin, and A. Fataruba, "Identification of chitosan beads from coconut crab patani variety using Fourier Transform Infrared Spectroscopy (FTIR)," in *Journal of Physics: Conference Series*, Vol. 1832, No. 1, 012014, 2021.

[101] Ramos, J. V. H., F. d. M. Morawski, T. M. H. Costa, S. L. P. Dias, E. V. Benvenutti, E. W. d. Menezes, and L. T. Arenas, "Mesoporous chitosan/silica hybrid material applied for development of electrochemical sensor for paracetamol in presence of dopamine," *Microporous and Mesoporous Materials*, Vol. 217, 109–118, 2015.

[102] Wang, L., S. Tricard, P. Yue, J. Zhao, J. Fang, and W. Shen, "Polypyrrole and graphene quantum dots @ Prussian Blue hybrid film on graphite felt electrodes: Application for amperometric determination of l-cysteine," *Biosensors and Bioelectronics*, Vol. 77, 1112–1118, 2016.

[103] Tashkhourian, J. and A. Dehbozorgi, "Determination of dopamine in the presence of ascorbic and uric acids by fluorometric method using graphene quantum dots," *Spectroscopy Letters*, Vol. 49, No. 5, 319–325, 2016.

[104] Kandra, R. and S. Bajpai, "Drug release study on chitosan carbon dot loaded chitosan polymer film for wound healing and drug delivery," *Journal of Drug Research and Development*, Vol. 6, No. 1, 2470–1009, 2020.

[105] Yan, Y., Q. Liu, X. Du, J. Qian, H. Mao, and K. Wang, "Visible light photoelectrochemical sensor for ultrasensitive determination of dopamine based on synergistic effect of graphene quantum dots and TiO_2 nanoparticles," *Analytica Chimica Acta*, Vol. 853, 258–264, 2015.

[106] Da Costa, R. S., W. F. Da Cunha, N. S. Pereira, and A. M. Ceschin, "An alternative route to obtain carbon quantum dots from photoluminescent materials in peat," *Materials*, Vol. 11, No. 9, 1492, 2018.

[107] Sadrolhosseini, A. R., G. Krishnan, S. Safie, M. Beygisangchin, S. A. Rashid, and S. W. Harun, "Enhancement of the fluorescence property of carbon quantum dots based on laser ablated gold nanoparticles to evaluate pyrene: Publisher's note," *Optical Materials Express*, Vol. 10, No. 10, 2705–2705, 2020.

[108] Bokare, A., D. Nordlund, C. Melendrez, R. Robinson, O. Keles, A. Wolcott, and F. Erogbogbo, "Surface functionality and formation mechanisms of carbon and graphene quantum dots," *Diamond and Related Materials*, Vol. 110, 108101, 2020.

[109] Tan, F., L. Cong, X. Li, Q. Zhao, H. Zhao, X. Quan, and J. Chen, "An electrochemical sensor based on molecularly imprinted polypyrrole/graphene quantum dots composite for detection of bisphenol A in water samples," *Sensors and Actuators B: Chemical*, Vol. 233, 599–606, 2016.

[110] Zhao, J., L. Zhao, C. Lan, and S. Zhao, "Graphene quantum dots as effective probes for label-free fluorescence detection of dopamine," *Sensors and Actuators B: Chemical*, Vol. 223, 246–251, 2016.

[111] Mohammadi, S., S. Mohammadi, and A. Salimi, "A 3D hydrogel based on chitosan and carbon dots for sensitive fluorescence detection of microRNA-21 in breast cancer cells," *Talanta*, Vol. 224, 121895, 2021.

[112] Yuan, X., Z. Liu, Z. Guo, Y. Ji, M. Jin, and X. Wang, "Cellular distribution and cytotoxicity of graphene quantum dots with different functional groups," *Nanoscale Research Letters*, Vol. 9, 1–9, 2014.

[113] Konwar, A., N. Gogoi, G. Majumdar, and D. Chowdhury, "Green chitosan-carbon dots nanocomposite hydrogel film with superior properties," *Carbohydrate Polymers*, Vol. 115, 238–245, 2015.

[114] Zavareh, H. S., M. Pourmadadi, A. Moradi, F. Yazdian, and M. Omidi, "Chitosan/carbon quantum dot/aptamer complex as a potential anticancer drug delivery system towards the release of 5-fluorouracil," *International Journal of Biological Macromolecules*, Vol. 165, 1422–1430, 2020.

[115] Roshidi, M. D. A., Y. W. Fen, W. M. E. M. M. Daniyal, N. A. S. Omar, and M. Zulholinda, "Structural and optical properties of chitosan–poly (amidoamine) dendrimer composite thin film for potential sensing pb^{2+} using an optical spectroscopy," *Optik*, Vol. 185, 351–358, 2019.

[116] Mathew, S. A., P. Praveena, S. Dhanavel, R. Manikandan, S. Senthilkumar, and A. Stephen, "Luminescent chitosan/carbon dots as an effective nano-drug carrier for neurodegenerative diseases," *RSC Advances*, Vol. 10, No. 41, 24 386–24 396, 2020.

[117] Chellasamy, G., S. R. Ankireddy, K.-N. Lee, S. Govindaraju, and K. Yun, "Smartphone-integrated colorimetric sensor array-based reader system and fluorometric detection of dopamine in male and female geriatric plasma by bluish-green fluorescent carbon quantum dots," *Materials Today Bio*, Vol. 12, 100168, 2021.